GLCX-011
September 2004

GLC X-BAND TECHNICAL NOTE

Accelerator Structure Developments for NLC/GLC

J. Wang
SLAC, Stanford Accelerator Center
2575 Sand Hill Rd., Menlo Park, CA 94025, USA

T. Higo
KEK, High Energy Accelerator Research Organization
1-1, Oho, Tsukuba, Ibaraki, 305-0801, Japan

Abstract

The NLC (Next Linear Collider) and GLC (Global Linear Collider) are e^+e^- linear collider proposals based on room-temperature accelerator technology – so called "warm machines" in comparison with TESLA "cold machine" that is based on super-conducting accelerator technology. There have been two major challenges in developing X-band (11.4GHz) accelerator structures for GLC/NLC. The first is to demonstrate stable, long-term operation at the high gradient (65MV/m) that is required to optimize the machine cost. The second is to strongly suppress the beam induced long-range wakefields, which is required to achieve high luminosity. The development of high gradient structures has been a high priority in recent years. Nearly thirty X-band structures with various rf parameters, cavity shapes and coupler types have been fabricated and tested since 2000. This program has been a successful collaborative effort among groups at SLAC, KEK, FNAL and other labs. A summary of the main achievements and experiences are presented in this paper as well as a status report on the structure design, high power performance, manufacturing techniques, and other structure related issues.

Submitted to ICFA Beam Dynamics Newsletter No.32, Feb., 2004.

2.2. Accelerator Structure Development for NLC/GLC

Juwen Wang
Stanford Linear Accelerator Center
Menlo Park, California, 94025, USA
mail to: jywap@SLAC.Stanford.EDU

Toshiyasu Higo
KEK, High Energy Accelerator Research Organization
1-1 Oho, Tsukuba, Ibaraki, 305-0801, Japan
mail to: toshiyasu.higo@kek.jp

2.2.1. Abstract

The NLC (Next Linear Collider) and GLC (Global Linear Collider) [1,2] are e^+ e^- linear collider proposals based on room-temperature accelerator technology – so called "warm machines" in comparison with the TESLA "cold machine" that is based on superconducting accelerator technology. There have been two major challenges in developing X-band (11.4 GHz) accelerator structures for the GLC/NLC. The first is to demonstrate stable, long-term operation at the high gradient (65 MV/m) that is required to optimize the machine cost. The second is to strongly suppress the beam induced long-range wakefields, which is required to achieve high luminosity. The development of high gradient structures has been a high priority in recent years. Nearly thirty X-band structures with various rf parameters, cavity shapes and coupler types have been fabricated and tested since 2000. This program has been a successful collaborative effort among groups at SLAC, KEK, FNAL and other labs. A summary of the main achievements and experiences are presented in this paper as well as a status report on the structure design, high power performance, manufacturing techniques, and other structure related issues.

2.2.2. Introduction

With the advent of the SLAC electron-positron linear collider in the 100 GeV center-of-mass energy range, research and development on even higher energy machines of this type started at several laboratories around the world. This research is motivated by the fact that linear colliders are the only viable approach to study e^+ e^- physics at center-of-mass energies approaching 1 TeV. As part of this effort, R&D on advanced accelerator structures at SLAC and KEK started in the late 1980's. The flow chart below provides a brief summary of the accelerator structure design progression that followed[3].

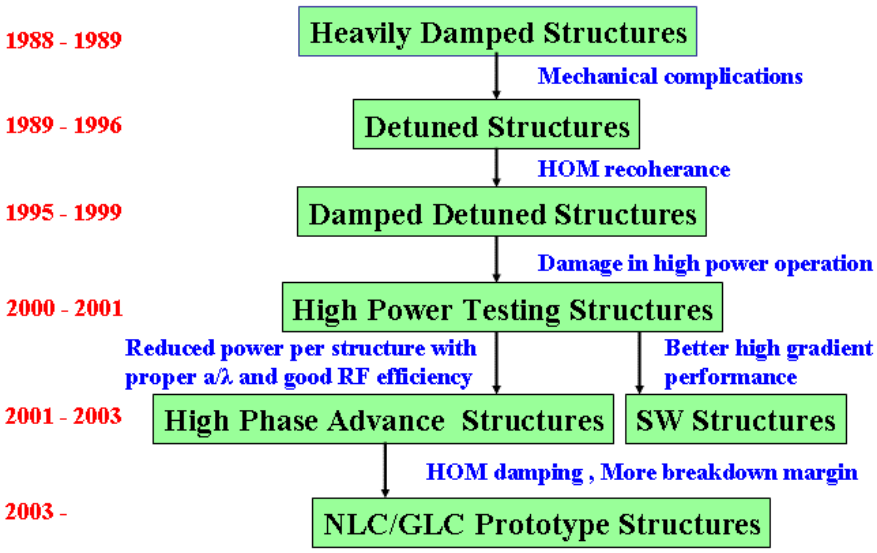

Figure 1. Brief history of accelerator structure R&D.

For X-Band (11.4 GHz) structures, the long-range transverse wakefield excited by the beam is relatively strong. These fields need to be reduced by about two-orders of magnitude within the 1.4ns bunch spacing. In the late 1980's, we developed two types of heavily damped structures: radial slots in the accelerator disks and circumferential slots in the side walls of the accelerator cavities. From computer simulations and cold tests of short cell stacks, dipole mode Q's as low as 10 seemed possible in both types of structures. However, due to the mechanical complications of making such structures, we instead switched to a detuning approach to suppress the wakefields. Detuning requires that each cell of the structure have a slightly different dipole frequency such that the net wakefield from the different modes decreases rapidly and smoothly during the period between bunches. Specifically, the dipole frequency is varied along the structure to produce a Gaussian distribution in the product of the mode density and the mode coupling strength to the beam.

Two 1.8m long Detuned Structures (DS1, DS2) with 10% Gaussian frequency detuning were produced initially. The prediction and measurement of the DS1 wakefield showed that the detuning produces an approximately Gaussian falloff in the net wakefield generated by each bunch, and works well to suppress the wakefield for about 30 ns, after which the amplitude increases due to a partial recoherence of the mode excitations. To offset this rise in the next generation of structures, weak mode damping was introduced by coupling each cell through longitudinal slots to four TE11 circular waveguides (manifolds) that run parallel to the structure. This reduces the dipole mode quality factors from about 6000 to 1000. By the late 1990's, several 1.8m Damped Detuned Structures (DDS1, DDS2 and DDS3) were fabricated and good agreement was achieved between the measured and predicted wakefields. This success had required advances in several areas including precision field calculations, machining and assembly procedures.

The final step in the design evolution was to optimize the cell shape to decrease the required power for a given gradient. This resulted in a rounded cell shape and the first

prototype Rounded Damped Detuned Structure (RDDS1) was fabricated to evaluate its performance. The design proved successful in improving efficiency. However, the high gradient studies that were ongoing at this time began to show serious gradient limitations with the basic 1.8m structure design, independent of the wakefield suppression features.

The high gradient testing has been done at the Next Linear Collider Test Accelerator (NLCTA), which was designed for RF system integration studies. Improvements to the power sources and operational capabilities in the late 1990's allowed more systematic studies at higher gradients. After high power operation, both RF measurements and visual inspections by boroscope revealed that the 1.8m structures were being damaged by rf breakdown. The net RF phase advance through the structures had increased by roughly 20 degrees per 1000 hours of operation at gradients as low as 50MV/m[4,5]. In 2000, we started an aggressive program to improve the high gradient performance of the structures. A large design parameter space was explored including different accelerator lengths, aperture sizes, group velocities, phase advances, and cavity types (standing-wave and traveling-wave). Also, improvements were made in the techniques used to clean and bake the structures before testing. Based on the experience gained from having tested nearly thirty structures, an optimal design has been selected that includes the wakefield suppression features originally developed for the 1.8m structures.

2.2.3. Structure Design

2.2.3.1. RF system configuration

The layout of an rf unit in the NLC/GLC linac is shown in Figure 2. Two 75 MW PPM klystrons with 1.6 μs pulses drive a dual-moded SLED-II pulse compression system to obtain 450 MW, 400 ns rf pulses. This power is then divided to feed eight, 60-cm long accelerator structures. The 56 MW of rf input power per structure produces an unloaded gradient of 65 MV/m.

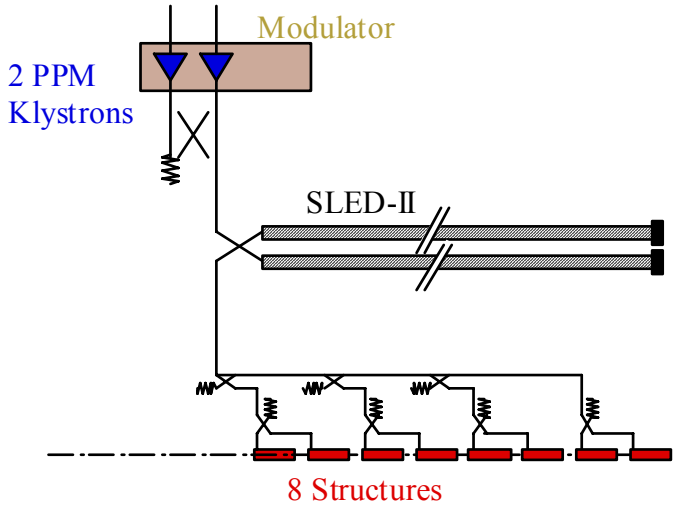

Figure 2. RF system configuration in the GLC/NLC main linac.

2.2.3.2. Basic RF parameters of the accelerator structures

The choice of operating frequency has a major influence on almost every aspect of linear collider design. The X-Band operating frequency (11.4 GHz) is believed to provide the major cost benefits of a high frequency RF system (high gradient with good efficiency and low RF energy per pulse) while still having achievable wakefield related alignment tolerances.

The choice of the average accelerator iris aperture, a, is a tradeoff between efficiency, where a small size is desired, and limits on the allowed short-range wakefield strength, which scales as $1/a^{3.5}$. As a compromise, values of a/λ of 0.17~0.18 have been chosen (λ is the rf wavelength). Also, a quasi-constant gradient traveling-wave structure design is used. Considering the multi-bunch beam loading, the accelerator attenuation factor, $\tau = 0.5\ln(P_{in}/P_{out})$, for optimal rf efficiency is 0.5 ~ 0.6, which corresponds to an rf filling time of 100 ~ 120 ns[6].

2.2.3.3. High phase advance accelerator structures

The first set of structures tested as part the high gradient program were low group velocity (0.03c ~ 0.05c) since the low-group velocity (downstream) portion of the 1.8m structures showed little damage. Although these structures proved much more robust, they have a smaller iris size ($a/\lambda = 0.13$) than required. Designing a low group velocity structure with $a/\lambda = 0.17 \sim 0.18$ is difficult since the simple solutions significantly lower the rf efficiency. The design that was adopted required increasing the phase advance per cell ($5\pi/6$ instead of $2\pi/3$) and using thicker irises to maintain a relatively high shunt impedance with the larger iris size. In order to maintain an optimal filling time, the structure length was scaled from the earlier 1.8m structures, which had group velocities of 0.12 c ~ 0.03 c, to a 0.6 m length with group velocities of 0.04 c ~ 0.01 c.

Table 1 lists the parameters for the most recent structure design. Note that this structure has pillbox-shaped cells. By optimally shaping the cell, as was done for RDDS1, the Q value and shunt impedance can be increased by about 10%.

Table 1. Basic structure parameters.

Structure name	HDDS (H60VG4SL17)
Structure length	62 cm (including couplers)
Number of acceleration cells	53 cells + 2 matching cells
Average cell iris radius	$< a/\lambda > = 0.17$
Phase advance / cell	$5\pi/6$
Group velocity	4.0 ~ 0.9 % speed of light
Attenuation parameter τ	0.64
Filling time	118 ns
Q value	7000 ~ 6500
Shunt impedance	51 ~ 68 MΩ/m
Coupler	Wave Guide type
1st Band dipole mode distribution	$Sech^{1.5}$ distribution with Δf~ 11% (4σ)
Es/Ea	2.22 – 2.05
Required input power	59 MW
Gradient without beam $<E_0>$	65 MV/m
Beam loaded gradient $<E_L>$	52 MV/m

2.2.3.4. Cavity dimension calculation

The parallel computing code Omega3P has been used to compute the cell dimensions for various accelerator structures[7]. The left half of Figure 3 shows the domain composition by color-coded meshes for a 16-parallel-processor simulation of one-eighth of an accelerator cavity with damping manifolds. The cavity frequency convergences as the fourth power of the mesh size. The Omega3P results agree with cold test measurements to within half a MHz for the 11424 MHz cavities, which is an accuracy well within the fabrication tolerances. The right half of Figure 3 shows the temperature increase due to rf pulse heating.

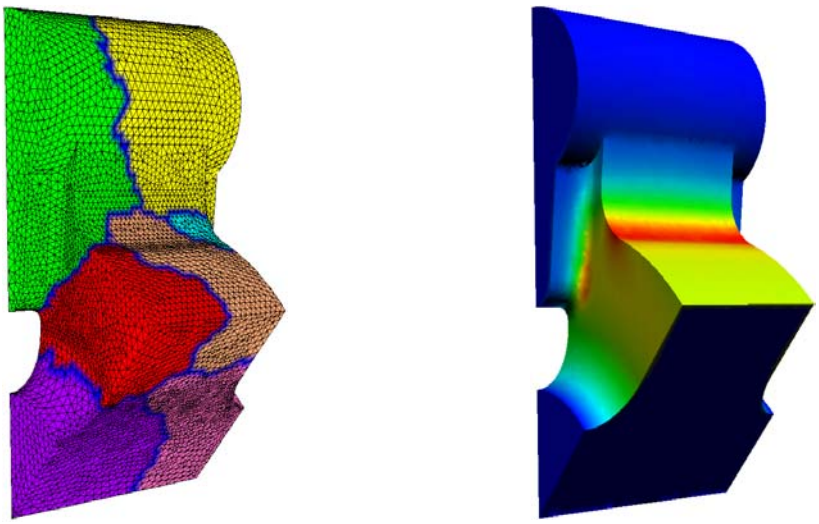

Figure 3. Meshes for parallel modeling (left) and illustration of pulse heating (right).

2.2.4. Wakefield Suppression

The manifold dipole mode damping scheme discussed above requires careful design to ensure the extracted energy flows out of the structure. At the ends of the structure, each manifold is connected to a rectangular waveguide through a coupling region followed by a 90 degree circular H bend, a taper to WR62 waveguide, and finally a manifold load with a coaxial probe for HOM signal monitoring. The matching quality for the propagating HOM frequencies of this assembly has a significant affect on the long-range wake. Figure 4 shows the HOM coupler layout used in computer simulations.

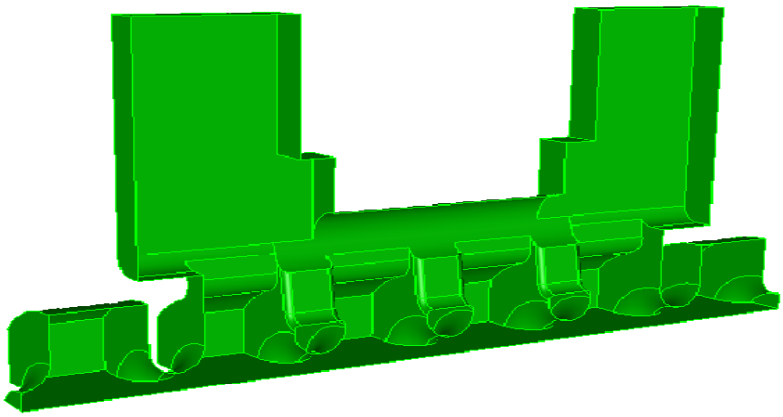

Figure 4. HOM coupler layout used in computer simulations.

The wakefield calculations are based on an equivalent circuit model that consists of a sequence of elements corresponding to the accelerator cells. Each cell is coupled to a transmission line representation of the HOM manifolds. All damped mode frequencies can be determined with this model. For moderate coupling to a manifold in our DDS structures, the modes are perturbed significantly and it becomes difficult and time consuming to calculate the wakefield from a modal summation. For this reason we

developed a Spectral Function Method.[8] The wakefield is expressed as a Fourier-like integral of a spectral function over the propagation band of the manifolds.

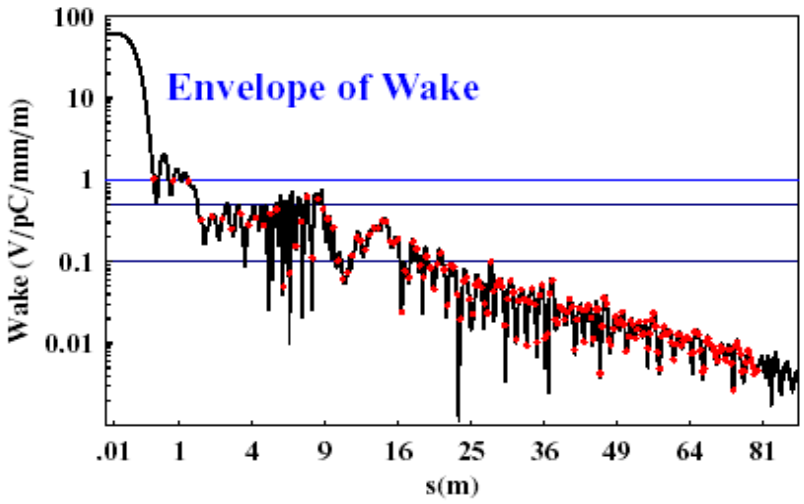

Figure 5. Calculated wakefield for recently designed HDDS structure. The dots indicate the locations of the bunches, which have a 1.4 ns spacing.

The wakefields for three of the damped and detuned structures have been measured at the ASSET facility in Sector 2 of the SLAC Linac[9]. Here, positrons extracted from the South Damping Ring serve as the drive bunch and electrons extracted from the North Damping Ring serve as the witness bunch. Figure 6 shows that a good agreement was achieved between the measurement and prediction for the RDDS1 structure. This structure has frequency errors in a few cavities near its center due to fabrication problems. These errors were estimated from bead-pull measurements of the fundamental mode. The wakefield is likely dominated by a few modes in the region of the cell errors, which can be corrected in the future. To realize the wakefield suppression afforded by the detuning also requires that the structure straightness be maintained (up to 100 micron peak-to-peak excursions are allowed). Such straightness has been routinely achieved in prototype structures.

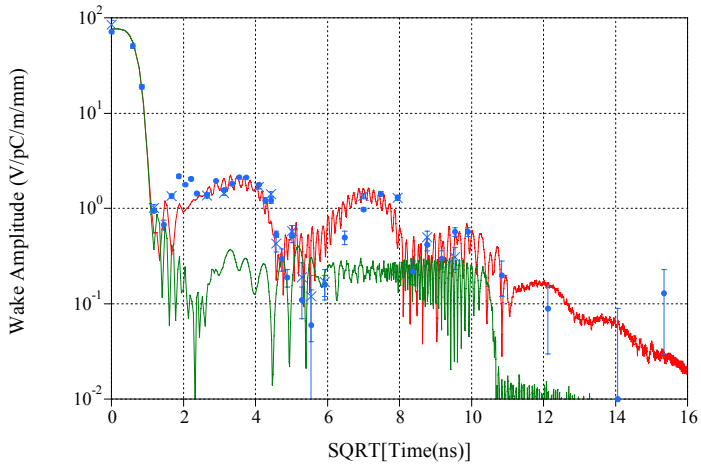

Figure 6. RDDS1 ASSET wakefield data (vertical = dots, horizontal = crosses) and prediction with (red) and without (green) known frequency errors.

Besides damping the dipole modes, the manifolds serve another useful function. Their signals provide a measure of the transverse position of the beam in the structure. Moreover, the beam coupling to the modes is fairly localized (2 to 10 cells) so filtering the signals by frequency yields beam offset information at different regions along the structure. As part of the wakefield measurement program, beam centering tests were done using dipole signals at two frequencies as a guide to position the drive beam. Measurements of the resulting short-range wakefield (< 300 ps) indicated that the drive beam had been centered to the 11 micron rms measurement accuracy, which was limited by the position jitter in the incoming beam. For comparison, the NLC/GLC goal is < 5 microns rms.

2.2.5. High Gradient Operation

Since the start of the linear collider program, much attention has been paid to the issue of high gradient performance. We were encouraged by tests in the early 1990's showing that unloaded gradients greater than 100 MV/m are possible and that the gradient limit increased with RF frequency. However, these tests were done with standing wave or low group velocity structures because high gradients were possible with the limited peak power available at that time. Later, higher group velocity structures (12% c in the first cell) were chosen for their lower cost and lower wakefields. However, these 1.8m structures failed to reach these high gradients and incurred significant breakdown related damage near their upstream ends at unloaded gradients of 45~50 MV/m with 240 ns pulses.

Stable high-field operation is very important since it affects the up-time of a linear colldier. For a 0.6 m structure, less than 1 breakdown per 2 million pulses is tolerable so as to rarely deplete the planned 2% overhead of rf units (this assumes a 10 second recovery time from a fault, which has been tested). In addition to the trip rate, there are limits on the copper erosion due to these breakdowns, which cause beam-to-rf-phase slip and reduce the energy gain. A rough guideline (less than 5% gradient reduction in 20 years of operation) imposes a criterion that the net phase advance change be less than 0.1 degrees per month of operation. From the small phase changes (typically 1 degree or less) that occur during the processing of the structures when there are thousands of breakdowns, we expect to meet this criterion if we extrapolate using the acceptable breakdown rate limit defined above.

2.2.5.1. Structure design optimization for efficiency and high gradient performance

After careful examination of GLC/NLC linac beam dynamics issues, we recently reduced the a/λ parameter for the structure design from 0.18 to 0.17. This change increases the structure efficiency by 10%, which reduces the required input power proportionally, and hence lowers the cost. Earlier studies also indicated that breakdown rates were lower with reduced input power, presumably because less 'collateral' damage is produced during breakdown. While this change increases the short-range wakefield by 20%, the increase is manageable. Another change that was made involves tailoring the gradient profile along the structures. We have seen that the breakdowns that occur after processing tend to be near the input end of the structure. Therefore, we have lowered the gradient at this end and increased it in output end while maintaining $a/\lambda = 0.17$ and a similar efficiency. Figure 7 shows the peak electric field profiles for different structure designs.

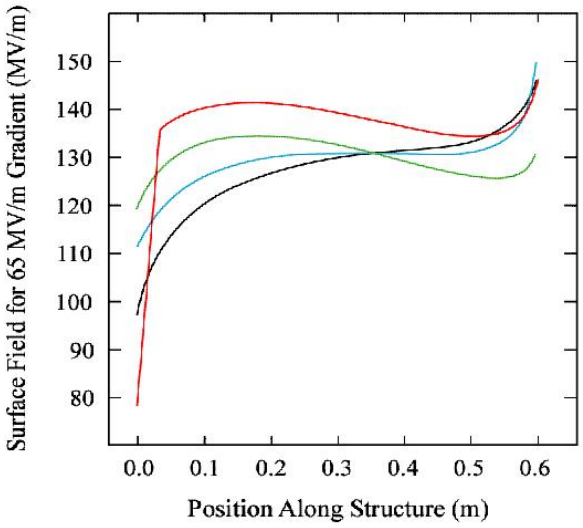

Figure 7. Comparison of maximum iris surface field for different structure designs at an unloaded gradient of 65 MV/m. The red curve is for H60VG3N (a/λ=0.18), which has rounded shaped irises – the others have elliptical shaped irises, which lowers the peak field. This structure also has a reduced field in the first several cells. The green curve is for H60VG3S18 (a/λ=0.18), which shows the effect of the elliptical shaped irises. The light blue curve is for H60VG3S17 (a/λ=0.17) and black curve is for the optimized H60VG4S17 (a/λ=0.17).

2.2.5.2. Structure input, output couplers and rounded coupling slots

During the early tests of low group velocity structures, the breakdown rate at high gradient was dominated by events in the input and output couplers. The rf signature of these events was different from those in the body and was similar from one structure to another. An autopsy of the input coupler of one of the structures revealed severe damage and some melting on the edges of the waveguide openings to the cell, and extensive pitting near these edges. The waveguide edges see large rf currents that are a strong function of their sharpness, and the associated pulse heating can be significant. By design, the edges in these structures were sharper (76μm radius) than those in the 1.8m structures (500μm radius), where this problem did not occur. The predicted pulse heating for the low group velocity structures was 130~170 °C, well below the copper melting point, but high enough to produce stress-induced cracking, which can enhance heating.

Several coupler designs that produce much lower pulse heating have been proposed[10]. Those shown in Figures 8(a) and 8(b) use rectangular-TE to circular-TM mode converters with different matching designs. Design (a) is referred to as a mode converter type and design (b) as a waveguide type. The pulse heating for both types of couplers is negligible.

Figure 8(c) shows an HDDS cell with pie-shaped slots to couple the dipole modes to the circular manifolds. The temperature rise due to rf pulse heating is reduced from 70^0C to about 25^0C by rounding the four slot edges with a 0.5mm radius and rounding the manifold openings to the accelerator cavities with a 2mm radius.

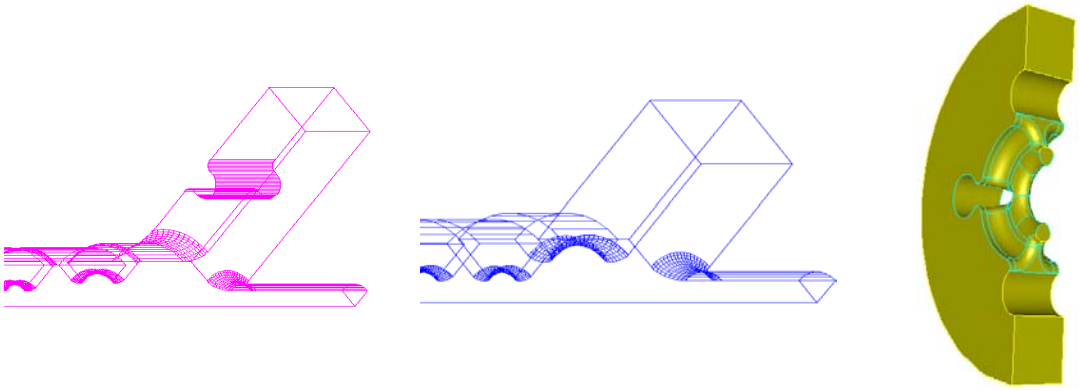

(a) (b) (c)

Figure 8. (a) and (b): Two types of rf couplers. (c): Rounded HOM coupling slots with low pulse heating.

2.2.5.3. High power test results

Since 2000, nearly thirty structures have been tested at the NLCTA shown in Figure 10(a) with over 15,000 hours of high power operation logged. The figure below summarizes the performance of the candidate structures tested in 2003. It shows the breakdown rate versus unloaded gradient during operation at the nominal 400 ns pulse width at a repetition rate of 60Hz. All of these structures have an acceptable average iris radius and dipole mode detuning. In addition, three of the structures (H60VG3-6C, H60VG3S18 and H60VG4S17-1) have slots (manifolds) in all or some of the cells to damp the long-range wakefield, consistent with GLC/NLC specifications. The observed variation in performance is due in part to variations in the design parameters as well as variations in the structure preparation methods, which are currently being refined. Some structures are also known to have problems that occurred during assembly and installation.

Although none of the structures meet the breakdown rate requirement of < 0.1 per hour at 65 MV/m, several do at 60 MV/m, and the average rate for all of these structures is acceptable at this gradient. While better performance is expected in future structures, these results already demonstrate the feasibility of a collider based on operation with an unloaded gradient of 60 MV/m. It should also be noted that, because of the field reduction from beam loading and the effective shortening of the pulse from the shaping required for beam loading compensation, the actual breakdown rates during beam operation at GLC/NLC will be smaller than those currently measured in tests with square pulses. The effect of the pulse shaping is shown by the two data points for the H60VG4S17-1 structure at 65MV/m.

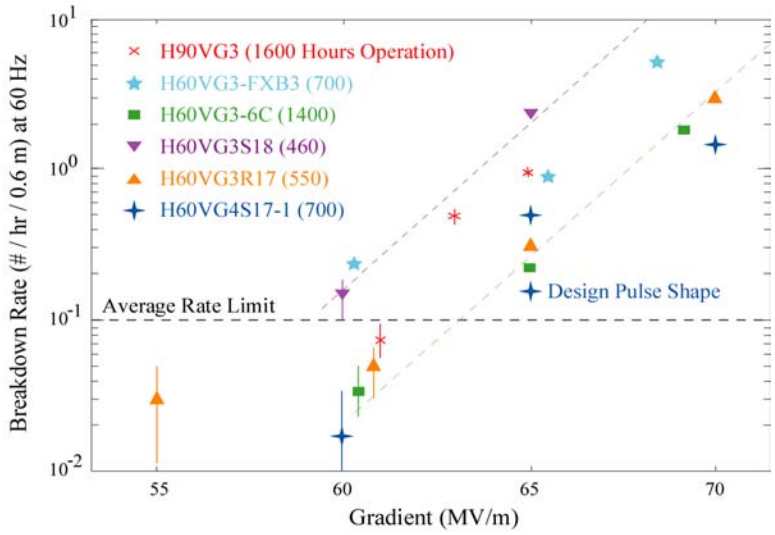

Figure 9. Breakdown rate as a function of unloaded gradient for several recently tested structures. The 'Design Pulse Shape' data point was taking with the ramped pulse that would be used in the NLC/GLC for beam loading compensation (square shaped pulses are normally used for testing as a worst case).

2.2.5.4. High power testing at KEK

A high power X-band rf system was recently re-established at KEK as shown in Figure 10(b). Structures having some of the designs listed in Figure 9 will be tested there starting in 2004. This program will help provide additional experience with high power operation of X-band accelerator structures. Eventually the facility will also allow us to conduct beam-related studies since its location was chosen to accept the ultra-low emittance beam that is extracted from the ATF (Accelerator Test Facility).

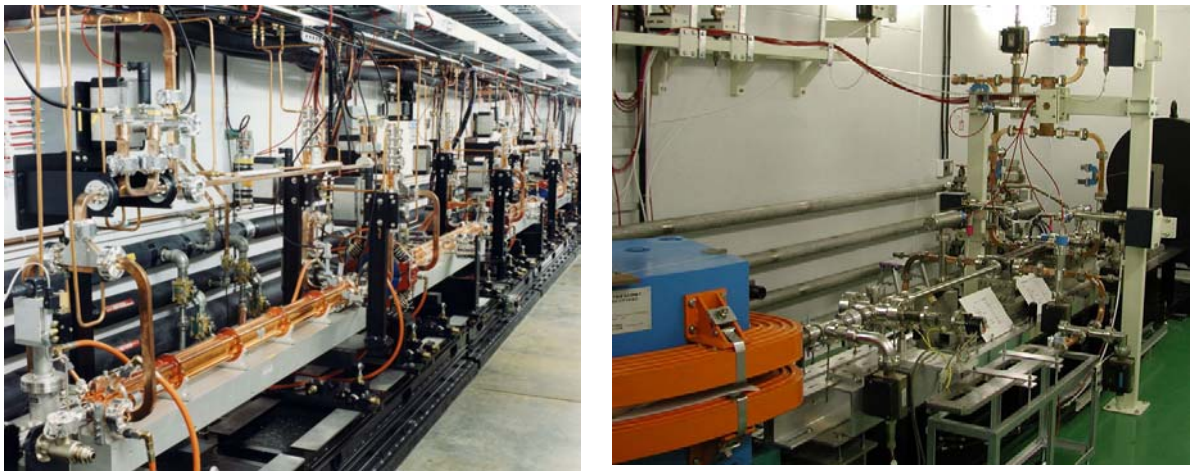

Figure 10: X-band high power test setup at SLAC and KEK.

2.2.6. Standing Wave Option

Standing-wave (SW) structures were considered for the NLC/GLC linacs because previous tests indicated they can operate at high gradients and they have the added benefit that they need only run at the loaded gradient. To explore this possibility, we built several 15-cell π-mode structures for evaluation. In all, four pairs of SW structures were tested[11]: two pairs of $a/\lambda = 0.18$ structures, one pair of higher a/λ structures and one pair of lower a/λ structures; these different a/λ designs would be used to produce piece-wise detuning of the dipole modes. Each pair of structures is fed from a high power 3db hybrid with a 90-degree phase difference in order to cancel the transient reflection back to the power source. After processing, the structures were operated at 55 MV/m, the GLC/NLC loaded gradient at the time (it is now 52 MV/m).

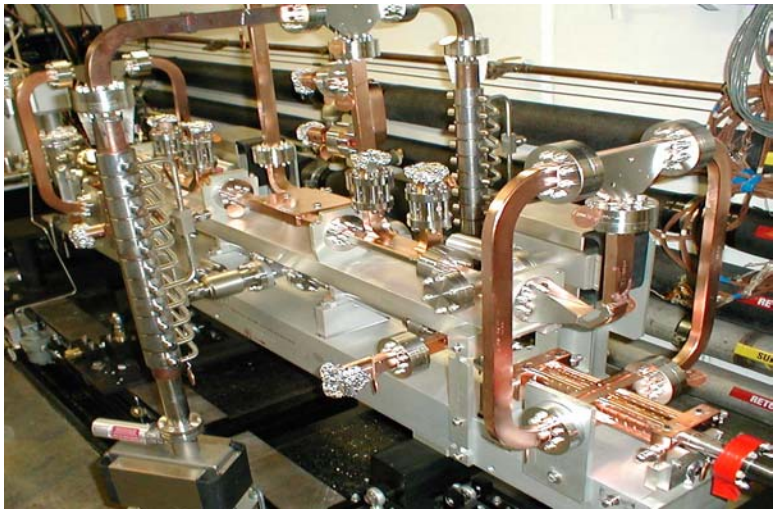

Figure 11. A pair of SW structures installed in the NLCTA beamline.

For two pairs of structures, the average breakdown rate at 55 MV/m was acceptable and no discernible shift in frequency was observed. However, at 60 MV/m the breakdown rate exceeded the acceptable limit, so they do not offer much more operating overhead than the present traveling wave structures. Also, damping the dipole modes in these structures is non-trivial and has not been tried. Currently, the development of these structures is on hold.

2.2.7. Other R&D

Besides the high gradient program, progress is also being made in improving the methods to suppress the long-range wakefield and in better understanding the various alignment and frequency tolerances. In addition, a wire-based method for measuring the wakefields is being developed so the time-consuming beam-based approach does not need to be used as often.

The long-range wakefield calculation program has been rewritten to automatically minimize the RMS and standard deviation of the sum wakefield (i.e. the net wakefield that would be seen by the 192 bunches). Another improvement involves the way detuning is applied to groups of structures, which is referred to as interleaving since the dipole frequencies are systematically offset structure to structure. This interleaving is necessary given that there are fewer modes in the shorter (60cm) structures to 'beat' against: the NLC/GLC linacs will probably use four-fold interleaving so there would be four unique

structure electrical designs. The improvement in this method has to do with making sure the actual modes are uniformly interleaved in frequency, not just the simple estimate of the mode frequencies that have been used in the past for design purposes. Finally, work is progressing to better define frequency and alignment tolerances. By simulating the emittance dilution of GLC/NLC bunch trains as they traverse the main linac, the cell-to-cell and the structure-to-structure frequency tolerances and alignment tolerances have been specified for both random and systematic errors. [12] Also, the structure bow tolerances and angle-offset tolerances are being carefully analyzed, and the contribution of higher frequency dipole bands to the wakefield are being evaluated.

A wire-based structure analysis method is being developed to quickly and inexpensively analyze the wakefield suppression properties of accelerator structures[13]. Using a 300-micron thick brass wire, measurements of the structure S-parameters are made to compute the impedances for the monopole band and higher dipole mode bands. The test results for a standing-wave structure, a short traveling-wave structure, and the RDDS1 structure show a reasonable agreement with computer simulations.

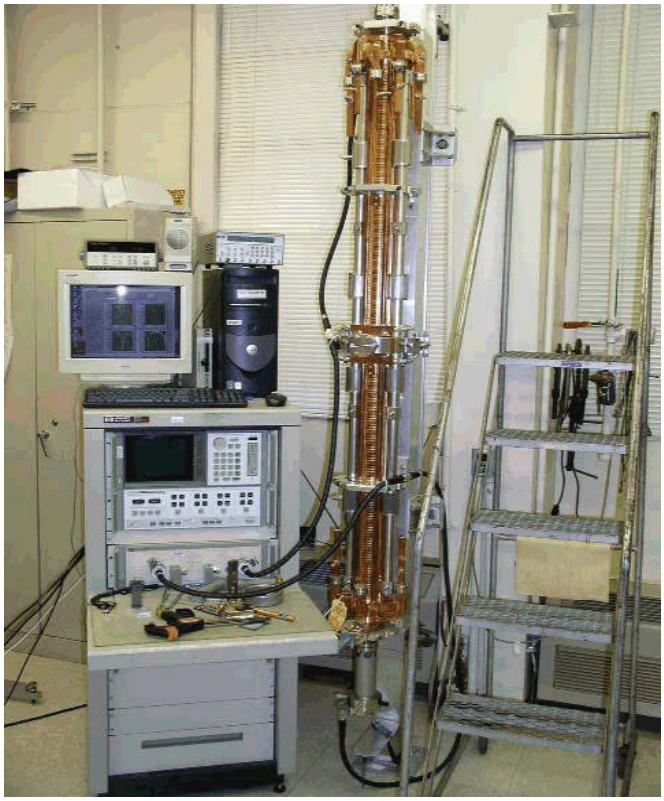

Figure 12. Wire measurement set-up with the RDDS1 Structure.

2.2.8. Structure Fabrication

Since early 1990's KEK has been a pioneering center for high-precision fabrication of structure cells using the diamond turning technique, which KEK originally introduced for fabrication of mirrors for use at SR light sources [14]. This high precision machining

technology, together with a variety of RF measurement techniques, allowed the NLC/GLC team to conduct a very precise validation of design calculations of the structure cells that involved complex 3-dimensional modeling. This program has been highly instrumental in advancing the designs of X-band accelerator structures.

2.2.8.1. Cell fabrication

Figure 13 shows a cell for the latest GLC/NLC accelerator structure. The material chosen is oxygen-free copper of grade-1, class-1, from which the cells are fabricated through a combination of precise milling and diamond turning.

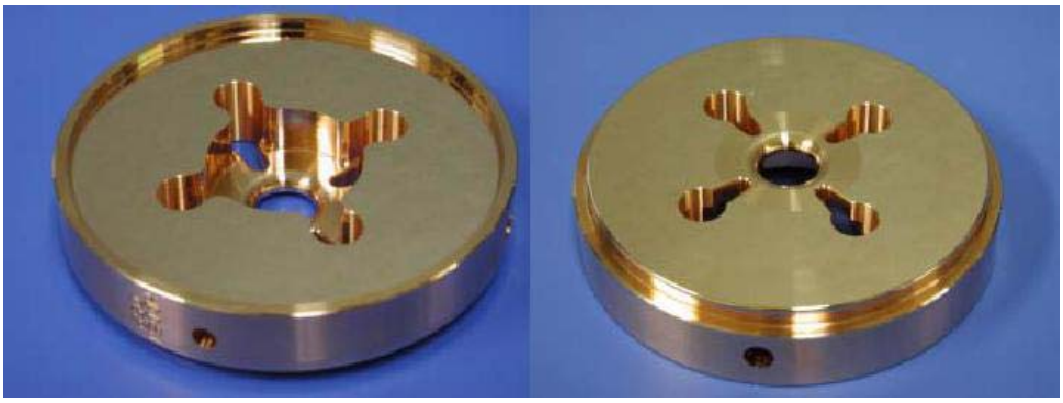

Figure 13. Photos of a HDDS cell.

Milling is required to create the slots and manifolds. Position control of about 10μm is required during milling to ensure proper mode frequencies as well as a smooth connection between the milled surfaces and the turned surfaces. The latter is required to avoid excessive surface heating during operation, which may lead to rf breakdown. Since a precision of this magnitude is readily available in industry, initial machining (so called "rough machining") of the cells, including milling, is done typically by outside contractors. The final cutting is done by using a diamond tool with a precision turning lathe which is placed in a temperature-controlled environment. The typical precision of 2μm in both the diameter and thickness can easily be obtained by using the following two procedures. The first is to measure the diameter of a cell after cutting, and apply corrections to the lathe set-up for the cutting of the later cells. This allows continual initialization of the radial position of the cutting tool. The second is the periodic cutting of the vacuum chuck surface with the diamond tool. This properly initializes the longitudinal position of the cutting tool. In addition, a few precautions specific to the accelerator cells need to be taken. For instance, since the material is very soft, excessive mechanical stress due to inadequate chucking and other forces must be avoided. While the dimensions inside the cavities are of critical importance in the light of precision control of the resonant rf frequencies, the outer features of the cell (for example, the surface flatness and outer diameter) also require attention since they determine the relative cell-to-cell alignment and bonding quality. These techniques, which were developed in the laboratory environment at KEK, are currently being transferred to industry. Typical specifications for the recent HDDS cells are summarized in the Table 2.

Table 2. Typical mechanical tolerances of a structure.

Item	Unit	Specification
Milling positioning	μm	10
Turning diameter	μm	2
Turning depth	μm	2
Tangential discontinuity	degree	5 or 8
Concentricity between milling and turning	μm	10
Concentricity of 2a, 2b and outer diameter	μm	1
Cell-to-cell alignment	μm	5 ~ 10

2.2.8.2.Frequency requirements

Many aspects of the electrical performance of accelerator structures are characterized by the resonant frequencies of individual cells. Of critical importance at GLC/NLC are the control of the fundamental mode (accelerating mode) resonance frequency f_0 and the lowest band dipole mode frequency f_1 in each cell. For adequate performance of accelerator structures at GLC/NLC in terms of wakefield detuning, the tolerance on f_1 is such that its rms random error stays below 3 MHz. As for f_0, the requirement of keeping the total phase slip of the fundamental mode along a structure within several degrees translates to a tolerance of ~0.1MHz for each cell. It is, however, not feasible to achieve this latter tolerance on f_0, unless one uses a feed-forward machining technique (to be discussed later) or resorts to post-assembly tuning. Thus, we impose an f_0 tolerance of ±1 MHz to dictate the machining tolerances, which can reasonably be realized by the present fabrication technology. This allows the issues of the total phase slip to be addressed in combination with suitable rf measurements as described later. If this is done, because of the known correlation between errors of f_0 and f_1 which arise from a variety of cell dimension errors, the associated errors of f_1 are expected to be within 2 ~ 3 MHz, which automatically satisfies the detuning requirement.

Extensive single and multi-disk rf measurements were made to verify the fundamental and dipole mode frequencies in the process of preparing RDDS1[15]. For single disk QC, each disk was sandwiched between two flat plates. The frequency deviation of four modes (fundamental zero and π mode, π mode of first dipole band and zero mode of second dipole band) were measured as shown in Figure 14. The rms deviations of the four sets of frequencies from smoothly varying curves is within 0.6 MHz.

Systematic errors in the fundamental frequency f_0 can be addressed in the following manner. First, it is known that an “average” f_0 of a “short stack” of disks (typically 6 disks in our experience), which correspond to a part of a completed accelerator structure, can be measured within ~ 0.2MHz. This allows us to estimate the average errors of f_0 with an adequate precision, so that if the accumulated phase error of the fundamental mode is predicted to exceed the desired value, 5 degrees for instance, one could perturb the cavity dimensions of subsequent cells to offset the systemic errors of previous cells. The most straightforward way of achieving this is to apply a correction in "b" (cavity radius) to the disks in later fabrication. A total integrated phase shift less than 3° for 2π/3 mode frequency was obtained for the RDDS1 structure.

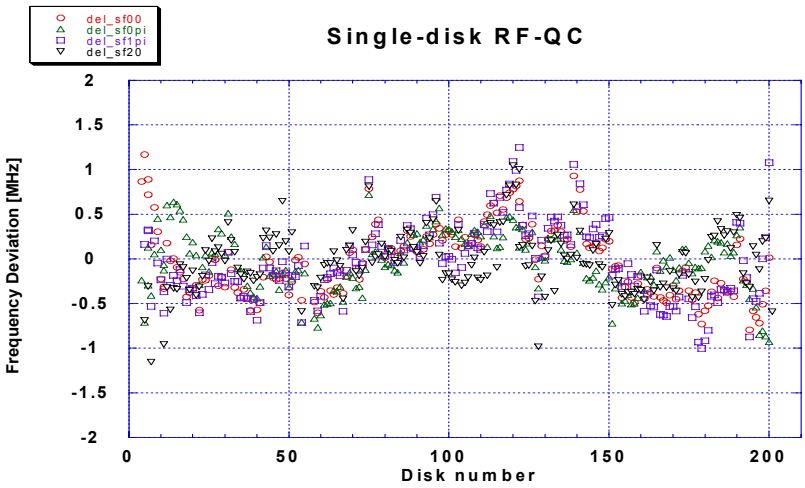

Figure 14. Four frequencies measured in a single-cell QC setup versus cell number.

In mass production environment this or other techniques may be employed to satisfy the tolerance on f_0 in addition to f_1. One may consider preparing a multiple set of cells with suitable rf measurements first, and select adequate ensembles of cells to build accelerator structures with the desired frequency distributions. One may also introduce "tuners" on the cells to do post-assembly frequency tuning. The exact choice of actions during cell fabrication, cell selection, structure assembly and rf measurements would depend on cost optimization in conjunction with the desired construction period and available mass production technology at the time of construction.

Of all these possibilities, a critical technological prerequisite is to fabricate the structure cells with a precision of ±1 MHz. However, it should be noted that this does not necessarily mean absolute control of all relevant dimensions. Rather, it requires the ability to make a contiguous set of cells with machining accuracy stable enough that the absolute frequency of a structure is maintained as a whole. The technology we have now is at the level listed in Table 2 and so is adequate. We know that the effect of a systematic error on higher mode frequencies from structure to structure in a linac is more severe than a random one. So we think that it is better to randomize the dipole frequencies among the structures in a linac by adding sub-micron offsets in the numerically controlled machining program.

2.2.8.3. Assembly through diffusion bonding

After fabrication, the cells are rinsed in an acid bath to remove the damaged layer from machining. The thickness of the layer removed is a few microns. These cells are subsequently stacked, guided by their outer diameter on a V-block, and are bonded in a copper-to-copper mutual diffusion process in a high-temperature (> 900°C) furnace. Here, a diffusion bonding technology was employed to assemble the structure body[16], while realizing the required alignment precision. The feasibility of this technology choice has been proven for the 1.8m RDDS1 structure. Stacking of cells on a V-block was good enough to obtain a cell-to-cell alignment at the micron rms level. After assembly, the bow of RDDS1 was about 200μm. Therefore, the bow of the present 60-cm-long structures should be an order of magnitude better, resulting in a much smaller bow than required.

2.2.8.4. Complete structure

All recent structure cells made by KEK were assembled and bonded at SLAC. In order to acquire the assembly and tuning experience at KEK, a program to complete full-size structures has been started. Recently KEK made a 60-cm-long structure, which is shown in Figure 15. The cells for this structure were machined and electrically inspected by a manufacturing company as a first step toward industrialization. The cells were chemically etched at KEK following the SLAC procedure. They were then bonded in a hydrogen furnace at 1020 °C for an hour at a local company. The bonding showed vacuum tightness, indicating that is possible to skip any brazing process for the main body. The couplers and some peripheral parts were integrated by brazing them in a hydrogen furnace. Finally, the structure at KEK was vacuum baked at 500 °C for a week in a double evacuation system. The structures at SLAC are wet and dry hydrogen fired, then vacuum baked at 650 °C for 2-3 weeks in a double evacuation system.

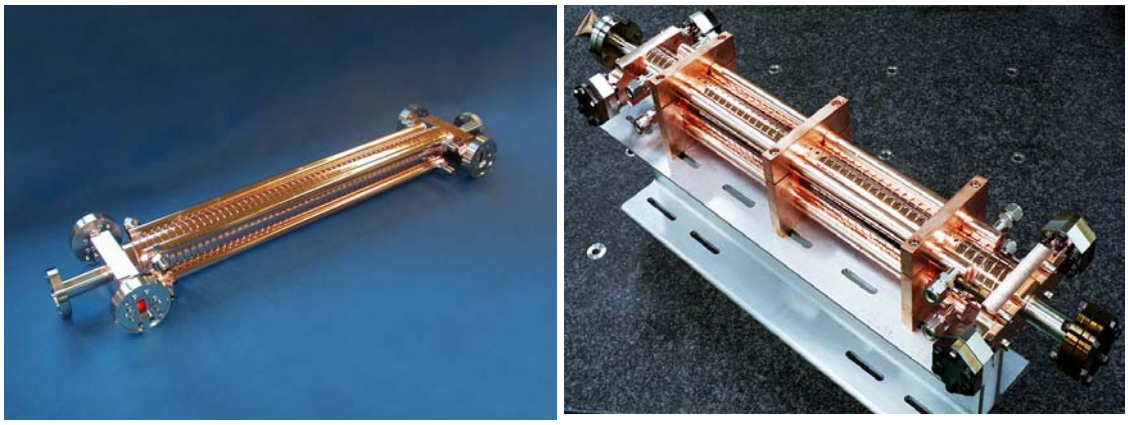

Figure 15. Recent 60 cm-long structure made by SLAC (left) and KEK (right).

2.2.9. Structure Fabrication at FNAL

The first structures built at Fermilab were proposed and designed by SLAC RF group. The initial goal of the Fermilab group was industrialization of NLC/GLC type structures. Subsequently, the RF group was formed and we developed extensive infrastructure (clean room, rf lab, vacuum furnaces, chemistry, tooling etc), and we have started to participate more extensively in structure development. We developed initial production techniques by making short 20cm long FXA structures, and we further honed the technology by building numerous 60cm long detuned structures (FXB series, or H60VG3R18) for high gradient testing. Five FXB's have been successfully tested at NLCTA. We have just completed development of the FXC structures (H60VG3S17), which incorporates damping and thus has all the features needed for the NLC/GLC. Our goals include: verification of SLAC's cell dimension table, design of input/output couplers, development of mechanical quality assurance, and rf quality control on each step of production including final tuning. Also, some effort will be spent on R&D on movable supports (girders), which constitute the basic cell in the main linac.

Recent FNAL structures differ in two basic ways from those produced by SLAC/KEK. One difference is that waveguide style couplers (Figure 8b) are used instead

of the mode converter style (Figure 8a). We designed the waveguide couplers to be more compact, and like the mode converter coupler, they have not been a problem during high gradient operation. Another difference is in the assembly and baking techniques used for the structures. We braze the cells together in a hydrogen-free environment at 780 degC while SLAC diffusion bonds the cells at 1020 degC in a hydrogen atmosphere. The idea is to avoid a high temperature exposure to hydrogen so a long vacuum bake is not required to remove it. Recent structures have also included a 1000 degC pre-bake of the cells to increase the grain sizes (we see some breakdown enhancement near grain boundaries), and to benefit from the surface conditioning that occurs when heating copper to a temperature near melting. All high temperature furnace heat treatments are done in a 500 mTorr partial pressure of argon to prevent copper sublimation. These changes have improved the high gradient performance of recent structures. For the FXC structures, a 3% hydrogen firing at 500 degC (in 500 mTorr Ar), followed by a three day full vacuum bake at 500 deg C is being performed to remove any copper oxide that may be present.

2.2.10. C-Band Development

The GLC team maintains a C-band main linac scheme (GLC-C) [2] as a possible backup option in addition to the X-band design. GLC-C features heavily damped, choke-mode structures[17] whose damping performance of the wakefield has been demonstrated in the past. The high-power operation of a GLC-C pulse compression was successfully tested at KEK in 2003. Since the SPring-8 Compact SASE Source (SCSS) program at RIKEN has adopted a C-band rf system which is basically identical to that of GLC-C, including the accelerator structure, it has been decided that many other aspects of the high-power feasibility studies concerning GLC-C would be studied in the course of the system development of SCSS. Figure 16 shows a setup at SPring-8 currently under preparation. A high field testing of a GLC-C accelerator structure is scheduled to take place in 2004.

Figure 16. High-power setup for C-band accelerator structure testing at SPring8.

2.2.11. Conclusions

An overview of the accelerator structure development efforts for the NLC/GLC have been presented. In summary:

- Computational techniques related to electrical designs are very mature. Likewise, practical design procedures for travelling wave structures are well advanced.

- Basic techniques for fabricating the cells within required precision are well established and are considered reasonable. In addition, a large amount of assembly experience has been accumulated. These techniques yield acceptable wakefield suppression as has been demonstrated.

- Full transfer of fabrication and assembly technologies to industry is believed doable and is in progress.

- Recent high-field testing shows the feasibility of a NLC/GLC with a 60 MV/m unloaded gradient. With additional improvements, the structure performance at 65 MV/m should also meet specifications. There is little cost difference (3 %) between machines based on either of these gradients.

2.2.12. Acknowledgements

We thank the present and former directors of SLAC and KEK for establishing and maintaining a formal R&D collaboration agreement on structure development. During the past 15 years, many people have contributed to the X-band structure program: they include C. Adolphsen, N. Baboi, K. Bane, G. Bowden, D.L. Burke, J. Cornuelle, V. Dolgashev, Z. Farkas, J. Frisch, E. Garwin, S. Harvey, H. Hoag, K. Jobe, R.M. Jones, R. Kirby, N. Kroll, F. Le Pimpec, Z. Li, G.A. Loew, J. Lewandowski, R.J. Loewen, D. McCormick, R.H. Miller, C. Nantista, J. Nelson, C.K. Ng, R. Palmer, E. Paterson, C. Pearson, N. Phinny, T. Raubenheimer, M. Ross, R.D. Ruth, T. Smith, S. Tantawi, K. Thompson, P.B. Wilson, **SLAC**. H. Baba, Y. Funahashi, N. Higashi, Y. Higashi, N. Hitomi, H. Kawamata, N. Kudo, T. Kume, H. Matsumoto, Y. Morozumi, J.S. Oh, T. Shintake, K. Takata, T. Takatomi, N. Toge, K. Ueno, Y. Watanabe, **KEK**. T. Arkan, C. Boffo, H. Carter, D. Finley, I. Gonin, T. Khabiboulline, S. Mishra, G. Romanov, N. Solyak, **FNAL**. J. Klingmann, K. van Bibber, **LLNL**. Finally, a special thanks to Chris Adolphsen and Nobu Toge for helping to edit this report.

2.2.13. References

[1] ISG Study Report, KEK-Report 2000-7 and SLAC R-559.

[2] GLC Project Report, KEK-Report-2003-7, also available from http://lcdev.kek.jp/ProjReport/.

[3] J. Wang, et al., Accelerator Structure R&D for Linear Colliders, PAC99, SLAC-REPRINT-1999-155.

[4] C. Adolphsen, et al. Processing studies of X-band accelerator Structures at NLCTA, PAC01, SLAC-PUB-8901.

[5] C. Adolphsen, Normal Conducting RF Structure Test Facilities and Results, PAC03, SLAC-PUB-9906.

[6] Z. Li, et al. Traveling Wave Structure Optimization for the NLC, PAC2001, SLAC-PUB-9049.

[7] Z. Li et al. RDDS Cell Design and Optimization for the Linear Collider Linacs, PAC99, SLAC REPRINT-1999-150.

[8] R. Jones, et al. A Spectral Function Method Applied to the Calculation of the Wake Function for the NLCTA, LINAC96, SLAC-PUB-7287.

[9] C. Adolphsen, et al. Measurement of Wake Field Suppression in a Damped Detuned Accelerator Structure, SLAC-PUB-7519, Phys. Rev. Lett. Vol 27, p2475, 1995.

[10] C. Nantista, et al. Novel Accelerator Structure Couplers, PAC2003, SLAC-PUB-10219.

[11] V. Dolgashev, et al. Status of X-Band Standing Wave Structure Studies at SLAC, PAC03, SLAC-PUB-10124.

[12] R. M. Jones, et al. Optimized Wakefield Suppression and Emittance Dilution Imposed Alignment Tolerances for the JLC/NLC, PAC03, SLAC-PUB-9868.

[13] N. Baboi, et al. Impedance Measurement Setup for Higher Order Mode Studies in NLC Accelerator Structures with Wire Method, LINAC 2002, SLAC-PUB-9472.

[14] Y. Higashi et al., Studies on High-precision Machining of Accelerator Disks of X-band Structure for a Linear Collider, KEK-Report 2000-1, 2000.

[15] T. Higo, et al. “Meeting Tight Frequency Requirement of Rounded Damped Detuned Structure”, Proceedings of the XX International Linac Conference, Monterey, USA, Aug., 2000.

[16] Y. Higashi et al, “Study on High-precision Diffusion Bonding for X-band Accelerator Structure”, KEK-Report 2000-2, 2000.

[17] C-band R&D, http://www-xfel.spring8.or.jp/.